Limnol. Oceanogr., 51(6), 2006, 2502–2514

Molecular analysis of photosynthetic picoeukaryote community structure along an Arabian Sea transect

Nicholas J. Fuller
Department of Biological Sciences, University of Warwick, Coventry, CV4 7AL, United Kingdom

Glen A. Tarran, Denise G. Cummings and E. Malcolm S. Woodward
Plymouth Marine Laboratory, Prospect Place, The Hoe, Plymouth, PL1 3DH, United Kingdom

Karen M. Orcutt[1]
Department of Biological Sciences, University of Warwick, Coventry, CV4 7AL, United Kingdom

Marian Yallop
School of Biological Sciences, University of Bristol, Bristol, BS8 1UG, United Kingdom

Florence Le Gall
Station Biologique de Roscoff, UMR 7127 CNRS et Université Pierre et Marie Curie, BP74, 29682 Roscoff, Cedex, France

David J. Scanlan[2]
Department of Biological Sciences, University of Warwick, Coventry, CV4 7AL, United Kingdom

Abstract

We developed oligonucleotide probes, based on plastid 16S ribosomal DNA (rDNA) sequences, to target 10 different algal classes (Chlorarachniophyceae, Chrysophyceae, Cryptophyceae, Eustigmatophyceae, Pavlovophyceae, Pelagophyceae, Pinguiophyceae, Prasinophyceae [clade VI], Prymnesiophyceae, and Trebouxiophyceae), for use with dot blot hybridization technology. These class-specific probes were then used to investigate the community structure of photosynthetic picoeukaryotes (<3 μm) along a transect in the Arabian Sea during September 2001, using hybridization to plastid 16S rDNA polymerase chain reaction amplicons. The transect ranged from oligotrophic open-ocean waters, just south of the Equator, through mesotrophic and eutrophic waters toward the north coast of Oman, crossing a region of monsoonal upwelling off the Omani northeast coast. Photosynthetic picoeukaryotes in the surface-mixed layer (SML) and deep chlorophyll maximum ranged from 1.0×10^3 cells mL^{-1} in southern oligotrophic waters to almost 30×10^3 cells mL^{-1} at the region of upwelling. Chrysophytes were abundant along most of the transect throughout much of the euphotic zone. Prymnesiophytes were abundant in surface waters along much of the transect. By contrast, trebouxiophytes were confined to deeper waters, below the SML. Pelagophytes were found in surface waters that were more mesotrophic, whereas cryptophytes were only detected in the more nutrient-rich waters at the northern end of the transect, between depths of 20–30 m. Pinguiophytes were also detected, but only in the warm surface waters off the north coast of Oman. Chlorarachniophytes, eustigmatophytes, pavlovophytes, and clade VI prasinophytes were essentially below detection limits for the entire transect.

Photosynthetic picoeukaryotes (PPEs), comprising cells <3 μm in size, are widely distributed in aquatic marine environments, and although numerically less abundant than their prokaryotic counterparts, *Prochlorococcus* and *Synechococcus*, they dominate the picophytoplankton biomass (e.g., *see* Blanchot et al. 2001; Worden et al. 2004). Moreover, the high cell-specific carbon (C)-fixation rates of these small eukaryotes has meant that they account for a large proportion of the picoplanktonic primary production (Li 1994). However, the morphological uniformity of this 'group' has hindered progress on establishing the dominant components of the PPE community and the distribution of key classes and genera in situ, important information given their significance in C cycling.

Pigment studies have been able to provide some idea of the distribution of PPEs in the marine environment. However, interpretation of the complex pigment patterns found in natural samples is made difficult by the fact that

[1] Present address: Darling Marine Center, University of Maine, Walpole, Maine 04573.
[2] Corresponding author (D.J.Scanlan@warwick.ac.uk).

Acknowledgments

We thank Jeff Benson at UKORS, National Oceanographic Centre, Southampton, for CTD data and Principal Scientist Peter Burkill, Captain Keith Avery, and crew of the RRS *Charles Darwin* for excellent logistical support on the AMBITION cruise. This work was supported by NERC grants NER/T/S/2000/00621 and GST/02/2819, the former as part of the Marine and Freshwater Microbial Biodiversity program. Support from the Plymouth Marine Laboratory core science program is also acknowledged.

most pigments are found in more than one algal class, while some are not necessarily present in every member of the same class. An exception is the pigment alloxanthin, which is restricted to the class Cryptophyceae, although it is not present in all members of this class. The carotenoid 19′-hexanoyloxyfucoxanthin (19HF) has been used to assess the presence of prymnesiophytes (Hooks et al. 1988), but this is complicated by the presence of 19HF in some dinoflagellates. Furthermore, although PPEs from many different classes have now been isolated from a variety of oceanographic locations (Vaulot et al. 2004), it is risky to extrapolate an abundance of a particular genus or class found in culture from a particular site to an actual abundance in situ, given the inherent selective nature of culture techniques.

It has been the recent advent of molecular approaches, however, that has led to most progress with regard to our understanding of the composition and distribution of the marine picoeukaryote community (*see* Diez et al. 2001; Moon-van der Staay et al. 2001; Not et al. 2004). Such studies, which have focused on use of the 18S ribosomal RNA (rRNA) gene, have revealed the dominance of prasinophytes, and particularly the genus *Micromonas*, especially in coastal marine waters. For more open-ocean environments, however, there is still a relative dearth of data pertaining to PPE community structure. Recently we developed a polymerase chain reaction (PCR) protocol biased toward recognizing marine algal plastids (Fuller et al. 2006), making it possible to assess more fully the PPE community in such regions where PPEs are less numerous, but nonetheless ecologically significant, members of the picophytoplankton community. In this study we report the development of plastid 16S rDNA-based probes for 10 algal classes, greatly expanding on the previous array of algal 18S rDNA molecular probes (Groben et al. 2004). In addition, we demonstrate the use of these probes to determine the in situ community structure of PPEs and reveal for the first time the complexity of this important community in an open-ocean environment along a transect in the Arabian Sea.

Materials and methods

Sampling—Seawater for DNA extraction was collected aboard the Royal Research Ship *Charles Darwin* (cruise CD132) along a transect in the Arabian Sea during September 2001 (Fig. 1; Table 1). Water was collected with a sampling CTD Rosette system comprising twenty-four 20-liter Niskin bottles on a hydrographic cable. Conductivity, temperature, and hydrostatic pressure were measured simultaneously with a CTD (model Sea-Bird 9/11) with additional fluorescence and oxygen detectors. Seawater (5 liters) was prefiltered through a 47-mm–diameter, 3-μm pore size filter (MCE MF-Millipore filters [Fisher]) and filtered onto a 47-mm–diameter, 0.45-μm pore size polysulphone filter (Supor® 450, 0.45 μm; Gelman Sciences) under gentle vacuum (10 mm Hg). The filter was placed in a 5-mL cryovial with 3 mL of DNA lysis buffer (0.75 mol L^{-1} sucrose, 400 mmol L^{-1} NaCl, 20 mmol L^{-1} ethylenediaminetetraacetic acid, and 50 mmol L^{-1} Tris-HCl [pH 9.0]) and stored at −80°C until extraction, as previously described (Fuller et al. 2003).

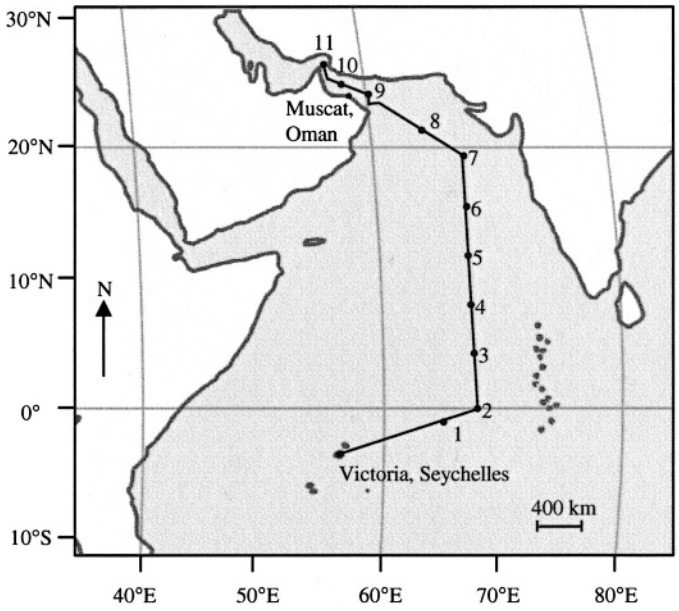

Fig. 1. Track of the transect sampled in the Arabian Sea, with station numbers marked.

Measurement of inorganic nutrients—Nitrate and soluble reactive phosphate were measured along the transect using a five-channel Technicon AAII, segmented flow colorimet-

Table 1. Stations sampled along the AMBITION cruise transect in the Arabian Sea.

Sta.	Coordinates	Date	Depths sampled (m)*
1	00°54.8′S, 064°8.5′E	03 Sep 01	10, 25, 50, 74, 100, 150
2	00°00.1′N, 066°59.7′E	05 Sep 01	10, 25, 50, 80, 100, 150
3	03°47.9′N, 067°00.0′E	07 Sep 01	10, 25, 55, 75, 110, 150
4	07°35.9′N, 067°00.3′E	11 Sep 01	10, 25, 50, 76, 100, 150
5	11°23.3′N, 067°00.0′E	13 Sep 01	10, 25, 50, 75, 150, 280
6	15°11.6′N, 067°00.0′E	15 Sep 01	10, 25, 44, 67, 80, 140, 200
7	19°00.1′N, 067°00.1′E	16 Sep 01	10, 25, 47, 80, 100, 130
8	20°55.3′N, 063°39.7′E	20 Sep 01	10, 28, 50, 80, 110, 150
9	23°33.7′N, 059°54.1′E	23 Sep 01	1, 9, 20, 30, 50, 100, 150
10	24°19.8′N, 058°10.4′E	25 Sep 01	10, 27, 50, 74, 100, 150
11	26°00.4′N, 056°35.2′E	27 Sep 01	1, 10, 27, 50, 70, 95

* Depths sampled for DNA extraction.

ric autoanalyzer. The chemical methodologies were applied as previously described for both nitrate (Brewer and Riley 1965) and phosphate (Kirkwood 1989). These techniques are summarized elsewhere (Woodward et al. 1999). The nanomolar ammonium system is an adaptation from Jones (1991), which uses a fluorescence analysis technique following ammonia gas diffusion out of the samples, passing across a hydrophobic Teflon membrane, due to pH differential chemistry. This cruise was the first deployment of a newly developed nanomolar detection-limit nutrient analyzer combining the sensitive segmented flow colorimetric analytical techniques with a Liquid Waveguide Capillary Cell detection system (Woodward 2002). All samples were taken and manipulated using 'clean' techniques (i.e., gloves were worn by the sampler and seawater was collected into acid-cleaned high-density polyethylene bottles, these being the first samples to be collected from each CTD cast) and were analyzed within 2 h of sampling. No samples were stored or frozen.

Flow cytometric analysis—Photosynthetic picoeukaryotes were enumerated from 2.2-mL seawater samples using a FACSort™ flow cytometer (Becton Dickinson). This analysis counted the cells in the samples and also measured chlorophyll fluorescence (>650 nm) and side scatter (light scattered at 90° to the plane of the vertically polarized argon ion laser exciting at 488 nm). Data acquisition was triggered on chlorophyll fluorescence, using laboratory cultures to set rejection gates for background noise. Samples were analyzed for 3 min at a flow rate of 95 $\pm$ 2.6 μL min^{-1}, and data were stored in 'listmode' format. The 'listmode' data were read using WinMDI Version 2.8 (Joseph Trotter) flow cytometry analysis software to produce scatter-plots of side scatter versus chlorophyll, from which cell counts were made.

Measurement of pigments—Bulk pigments (without prefiltration) from the Arabian Sea were measured by reverse-phase high-performance liquid chromatography, following a previously described method (Barlow et al. 1997).

Oligonucleotide probes—16S rDNA oligonucleotide probes were designed using the ARB program (Ludwig et al. 2004) and labeled with ^{32}P, as previously described (Fuller et al. 2003).

PCR amplification—Amplification of 16S rRNA genes from control strains (for dot blot hybridization) used the oxygenic phototroph-specific primers OXY359F (Nübel et al. 1997) and OXY1313R (West et al. 2001), following the PCR protocol described previously (Fuller et al. 2003). Amplification from environmental DNA for dot blot hybridization used a marine algal plastid-biased primer that we have recently developed, PLA491F (5′-GAGGAA-TAAGCATCGGCTAA-3′) (Fuller et al. 2006), in conjunction with OXY1313R, giving rise to an approximately 830–base pair PCR product. PCR amplification with the PLA491F–OXY1313R primer pair was carried out in a total reaction volume of 100 μL containing 200 μmol L^{-1} concentrations of deoxynucleotide triphosphates, 1.2 mmol L^{-1} $MgCl_2$, 0.2 μmol L^{-1} concentrations of primers, and 2.5 U of *Taq* polymerase in 1× enzyme buffer (Fermentas Life Sciences), with 1 mg mL^{-1} of bovine serum albumin (Roche). Amplification conditions comprised 95°C for 5 min and 80°C for 1 min, at which time *Taq* polymerase was added, followed by 30 cycles of 95°C for 30 s, 60°C for 30 s, and 72°C for 40 s, with a final extension at 72°C for 6 min. Two rounds of PCR were required to generate sufficient product for dot blot hybridization, using a dilution of the first product (0.5 ng) as template for the second round.

Dot blot hybridization—16S rDNA amplicons from Arabian Sea environmental DNA and from control strains were purified, blotted onto nylon membranes, and hybridized to algal class-specific oligonucleotide probes, following the method of Fuller et al. (2003, 2005). Final wash (or dissociation) temperatures (T_d) for each probe were determined empirically, following the method previously described (Fuller et al. 2003), and together with probe sequences, temperatures are shown in Table 2. Hybridization was quantified by using a Fujifilm FLA-5000 phosphorimager and Total Lab software (Phoretix). Relative hybridization of the PPE class-specific probes to total oxygenic phototroph 16S rDNA sequences amplified by the PLA491F–OXY1313R primer pair was calculated according to the equation below:

$$\text{Relative hybridization (\%)} = \left[\left(\frac{\text{S}env}{\text{E}env}\right) \cdot \left(\frac{\text{S}con}{\text{E}con}\right)^{-1}\right] \times 100$$

where S*env* and E*env* represent hybridization to environmental DNA of the specific and eubacterial probes, respectively, and where S*con* and E*con* are the slopes of the specific and eubacterial probe-binding curves, respectively, calculated by hybridizing each probe to dilution series of homogeneous control DNAs. The relative hybridization of a given specific probe, compared with that of the eubacterial probe, to the control DNAs was averaged where more than one control DNA was used.

Construction of contour plots—Arabian Sea data of physical, chemical, and biotic parameters were plotted as contour plots using Sigma Plot (version 8.0) software. Data were interpolated using the running average method with 0.01 sampling proportion and with "nearest neighbors" as the bandwidth method.

Statistical analyses—Multivariate redundancy analysis (RDA; Ter Braak 1994) was carried out to explore relationships between the environmental (explanatory) variables and the biotic (response) variables (PLA491F–OXY1313R dot blot relative hybridization values [%]), using the computer program CANOCO 3.1 (Ter Braak 1987, 1990). Two biotic variables, Pavlovophyceae and Chlorarachniophyceae, were excluded from the analyses as they were below detection limits. Explanatory variables included downwelling photosynthetically active radiation,

Table 2. 16 S rDNA oligonucleotide probes used in this study. T_d indicates dissociation temperature.

Probe	T_d (°C)	Sequence (5′-3′)	Target organisms	Reference
CHLA768	49	CCA TTC TCT CCC CTC GCT	Chlorarachniophyceae	This study
CHRY1037	52	GCA CCA CCT GTG TAA GAG	Chrysophyceae	This study
CRYP862	42	GGA TAC TTA ACG CCT TAG	Cryptophyceae	This study
EUB908	35	CCG TCA ATT CCT TTG AGT TT	Eubacteria	(Edwards et al. 1989)
EUST985	49	CAC TTC TAG CAA ACC CTG	Eustigmatophyceae	This study
PAVL665	37	TAG AAA TTC CTC CTA CCC	Pavlovophyceae	This study
PELA1035	52	ACC ACC TGT GTG TGT CTA	Pelagophyceae	This study
PING1024	47	ACG TAT TCC TTA CGG CAC	Pinguiophyceae	This study
PRAS826	58	GAT TCG CGT ATC CCC TAG	Prasinophyceae clade VI	This study
PRYM666	43	CTA GAA ATT CCC TCT ACC	Prymnesiophyceae	This study
TREB708	44	CCT TTG GTG TTC CTC CCG	Trebouxiophyceae (CCMP243, RCC9, and *Prototheca* clusters)	This study

dissolved oxygen, soluble reactive phosphate, salinity, temperature, and total oxidizable nitrogen. Explanatory variables were log (n + 1) transformed prior to analysis, as these variables were measured on different scales. A Forward Selection option was selected to rank explanatory variables in terms of their importance for explaining the spread of the species data. Response variables were square-root transformed prior to analysis to reduce the variance. Statistical significance of selected variables was determined by a Monte Carlo permutation test. Only those variables with a p value of <0.05 have been included. Spearman's rank correlations were calculated to explore the relationship between the PPE dot blot hybridization values and bulk pigment concentrations. Bonferroni corrections were applied to probability values to allow for multiple correlations.

Results

Probe development—We recently obtained 65 plastid 16S rDNA sequences from 14 algal classes (Fuller et al. 2006), and by comparing alignments of all available plastid 16S rDNA sequences, variable regions were identified that allowed oligonucleotide probes to be designed to target 10 different algal classes specifically (Table 2). The specificities of the probes were checked in silico by using the ARB sequence database tools and by performing BLAST searches (Altschul et al. 1997). CHLA768, PAVL665, and PING1024 specifically target all known chlorarachniophyte, pavlovophyte, and pinguiophyte sequences, respectively. The class Prasinophyceae comprises at least seven clades (Guillou et al. 2004), and probe PRAS826 specifically recognizes clade VI, which includes the genus *Prasinoderma*. CHRY1037 targets with no mismatches all known chrysophyte sequences, except the marine chrysophyte *Ochromonas distigma* RCC21 and the freshwater clone TLM14, which have a single mismatch. CRYP862 targets all known cryptophyte sequences, again with no mismatches, except for the environmental clone 34 w (from a saline meromictic lake), which has a single mismatch. However, in addition to recognizing cryptophytes, CRYP862 also targets marine dinoflagellates of the genus *Dinophysis*, which, according to plastid 16S rDNA phylogeny, are known to fall within the cryptophyte lineage (Hackett et al. 2003; Takahashi et al. 2005). Probe EUST985 specifically recognizes all known eustigmatophyte sequences except for the soil clone Dpcom253, which has three mismatches. Similarly, PELA1035 recognizes all known pelagophyte sequences except for *Ankylochrysis lutea* RCC286 and the marine clone OM164, which have two mismatches. PRYM666 targets all known prymnesiophytes except for the marine clone OM270 and the novel clade of Arabian Sea clones containing, for example, AS2_50C3 (Fuller et al. 2006), which have a single mismatch. TREB708 only targets the trebouxiophyte clusters containing *Chlorella vulgaris*, *Chlorella autotrophica* CCMP243, *Nannochloris* sp. RCC9 (but not *Nannochlorum eucaryotum*, which has two deletions), *Koliella spiculoformis*, and *Prototheca* spp. However, all known marine representatives of the trebouxiophytes are detected by this probe.

Specificity was confirmed experimentally by hybridization of the probes to dot blots containing 16S rDNA amplicons from different nontarget algal strains (Fig. 2). None of the probes hybridized significantly to nontarget strains except for PAVL665, which showed some cross-hybridization to a clade VI prasinophyte strain.

Arabian Sea transect: physical and chemical profiles—Examination of the temperature (Fig. 3A) and nutrient (Fig. 3C,D) profiles of the Arabian Sea transect revealed strong stratification, with warmer, lower-nutrient waters at the surface and cooler, more nutrient-rich waters below the thermocline. The depth of the surface mixed layer (SML) and thermocline was generally deeper in the southern part of the transect, and, in particular, the region of upwelling off the northeast coast of Oman can be clearly seen at and around Sta. 9, bringing cooler, nutrient-rich waters to the surface. A clear gradation can be seen from the southern stations, where especially nitrate (Fig. 3C), but also phosphate (Fig. 3D), concentrations in the surface waters were very low (around 10 nmol L^{-1} and 20–200 nmol L^{-1}, respectively), to the northern stations, where concentrations in surface waters for both nutrients were much higher. Surface waters also varied in their temperature, with the general trend of warmer waters in the south. However, surface waters at the northern tip of the transect, in the

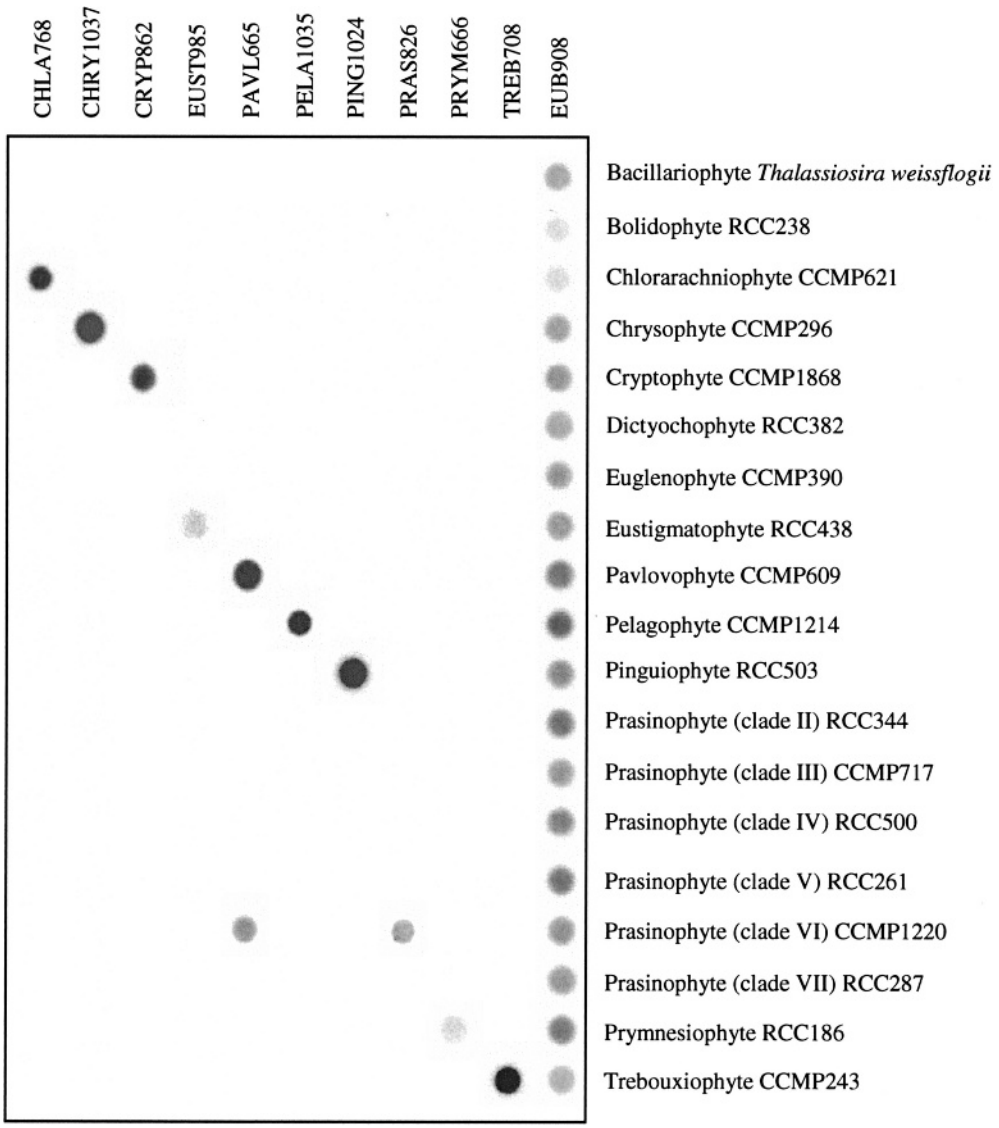

Fig. 2. Representative dot blots showing the specificity of hybridization of each algal class-specific oligonucleotide to arrays of control 16S rDNA amplicons.

Gulf of Oman, were especially warm (31.6°C), with coincident higher salinities (Fig. 3B).

Phytoplankton abundance—The profile of chlorophyll *a* (Chl *a*) along the Arabian Sea transect (Fig. 4A) shows the positioning of the deep chlorophyll maximum (DCM), just below the SML (Fig. 3A). Chl *a* concentration generally increased from south to north, with very high concentrations at Sta. 9 and 10, reaching 4.7 mg m^{-3} at Sta. 10. Flow cytometric enumeration of PPEs (Fig. 4B) revealed the highest abundance generally at the DCM in the oligotrophic south, but above the DCM, nearest the surface in the more nutrient-rich waters further north. Peak PPE abundance was found just above the nutricline throughout the transect and generally became shallower further north, where nutrients were found closer to the surface. Two noticeable peaks in abundance of PPEs were observed, at the Sta. 4 DCM (1.6×10^4 cells mL^{-1}) and the surface waters of Sta. 9 (2.9×10^4 cells mL^{-1}).

Bulk pigments—Pigment concentrations, while not being restricted to PPEs, were used to provide information on the groups of phytoplankton present along the transect. The distribution of the carotenoid alloxanthin, present only in cryptophytes, was observed throughout the transect at the DCM, generally matching the distribution of Chl *a* (Fig. 5A). However, the highest values of alloxanthin were observed not only at the DCM of Sta. 9 but also at the DCM of Sta. 11. The carotenoid 19HF, present only in prymnesiophytes and some dinoflagellates, was more evenly distributed over the transect, though still at greater concentrations at the DCM (Fig. 5B). The maximum concentration of 19HF was at the DCM of Sta. 8. The carotenoid 19′-butanoyloxyfucoxanthin (19BF), present in

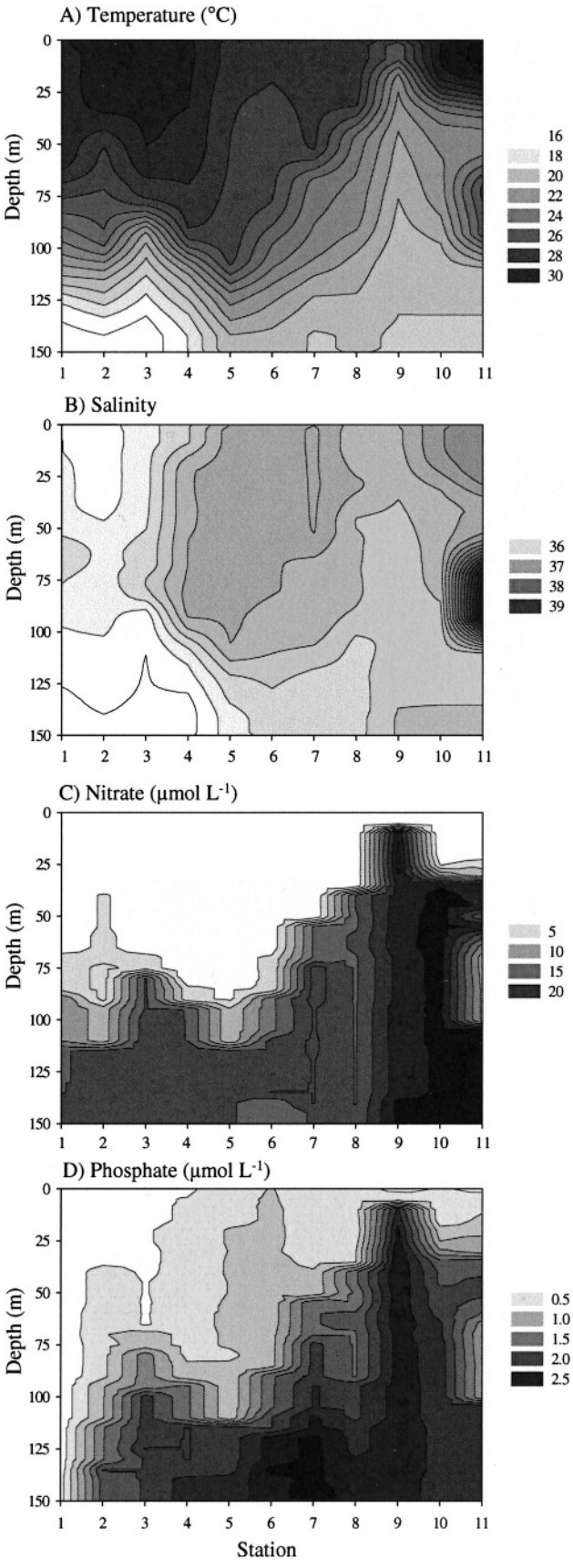

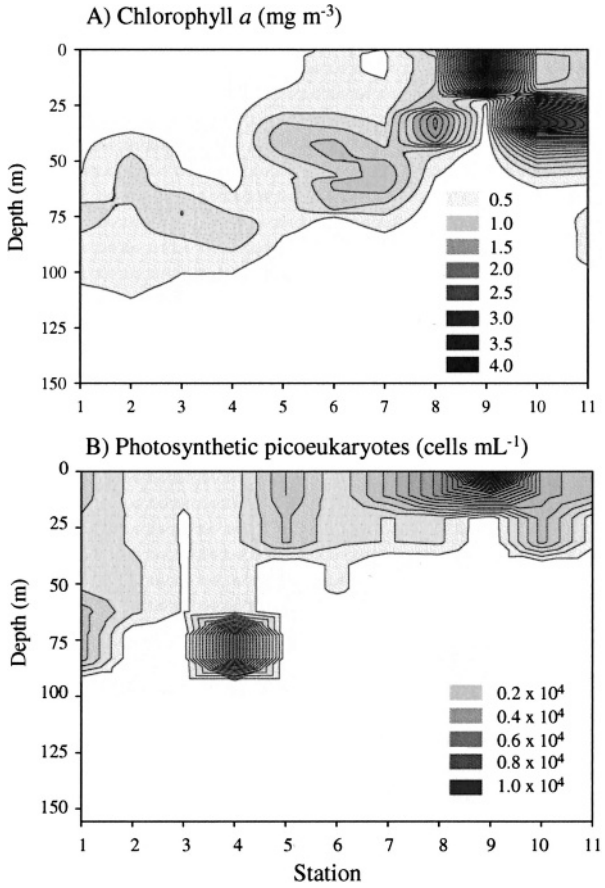

Fig. 4. Contour plots of the Arabian Sea transect, from Sta. 1 in the south to Sta. 11 in the north, of (A) chlorophyll *a* and (B) photosynthetic picoeukaryotes.

pelagophytes, dictyochophytes, some prymnesiophytes, some dinoflagellates, and one chrysophyte, also had a similar distribution to Chl *a*, though with a proportionately greater peak at the Sta. 8 DCM (Fig. 5C). The carotenoid fucoxanthin, present in diatoms, prymnesiophytes, chrysophytes, raphidophytes, pelagophytes, phaeophytes, pinguiophytes, and several dinoflagellates, also had a similar distribution to Chl *a*, but with a proportionately greater peak at the Sta. 9 DCM (Fig. 5D). The detection of the carotenoids violaxanthin, present in chlorophytes, prasinophytes, eustigmatophytes, pinguiophytes, and phaeophytes (Fig. 5E), and peridinin, present only in most dinoflagellates (Fig. 5F), throughout the transect also indicates the presence of some, or all, of these algal classes.

Photosynthetic picoeukaryotes—Dot blot hybridization of class-specific oligonucleotide probes to algal plastid 16S rDNA PCR products revealed the existence of PPEs from

←

Fig. 3. Contour plots of the Arabian Sea transect, from Sta. 1 in the south to Sta. 11 in the north, of (A) temperature, (B) salinity, (C) nitrate, and (D) phosphate concentration.

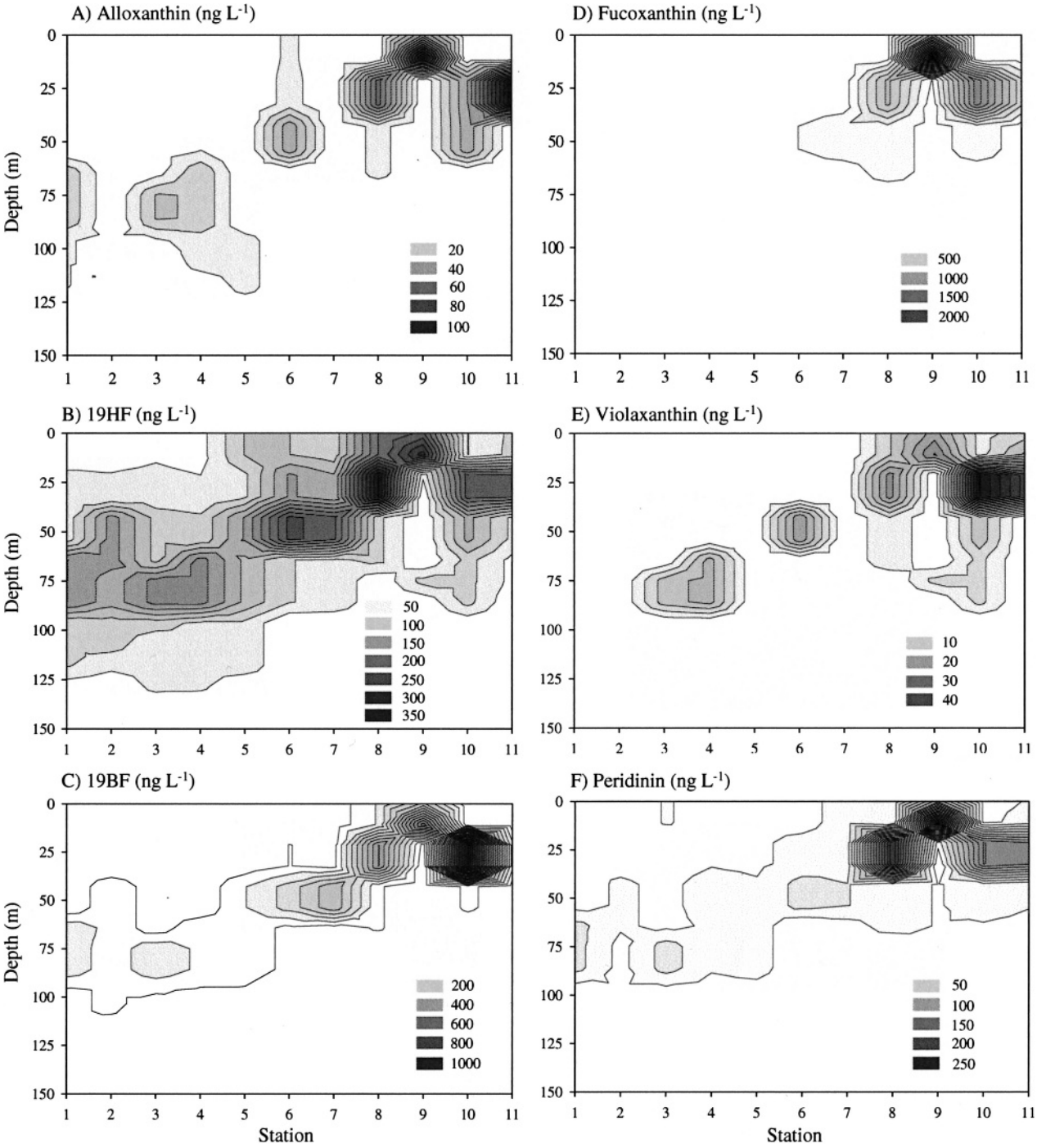

Fig. 5. Contour plots of the Arabian Sea transect, from Sta. 1 in the south to Sta. 11 in the north, of the pigments (A) alloxanthin, (B) 19HF, (C) 19BF, (D) fucoxanthin, (E) violaxanthin, and (F) peridinin.

several algal classes along the Arabian Sea transect (Fig. 6). Chrysophytes were abundant throughout most of the euphotic zone across the entire transect, though they generally gave a greater signal nearer the surface. Chrysophytes contributed the greatest proportion to the total signal of any algal class for most of the transect (Fig. 6A). In particular, in the surface waters of Sta. 10 they contributed 96.6% ± 5.7% of the total algal signal. Cryptophytes, by comparison, while having a much lower signal, had a much more restricted distribution, being generally confined to waters between 20 and 30 m in depth at the higher-nutrient and coastal Sta. 9 to 11 (Fig. 6B). Their maximum signal was at 27 m at Sta. 11 (4.9% ± 0.1%). Pelagophytes were largely confined to surface waters of the more mesotrophic region of the transect, from Sta. 5 to 8 (Fig. 6C), with a maximum signal in surface waters of

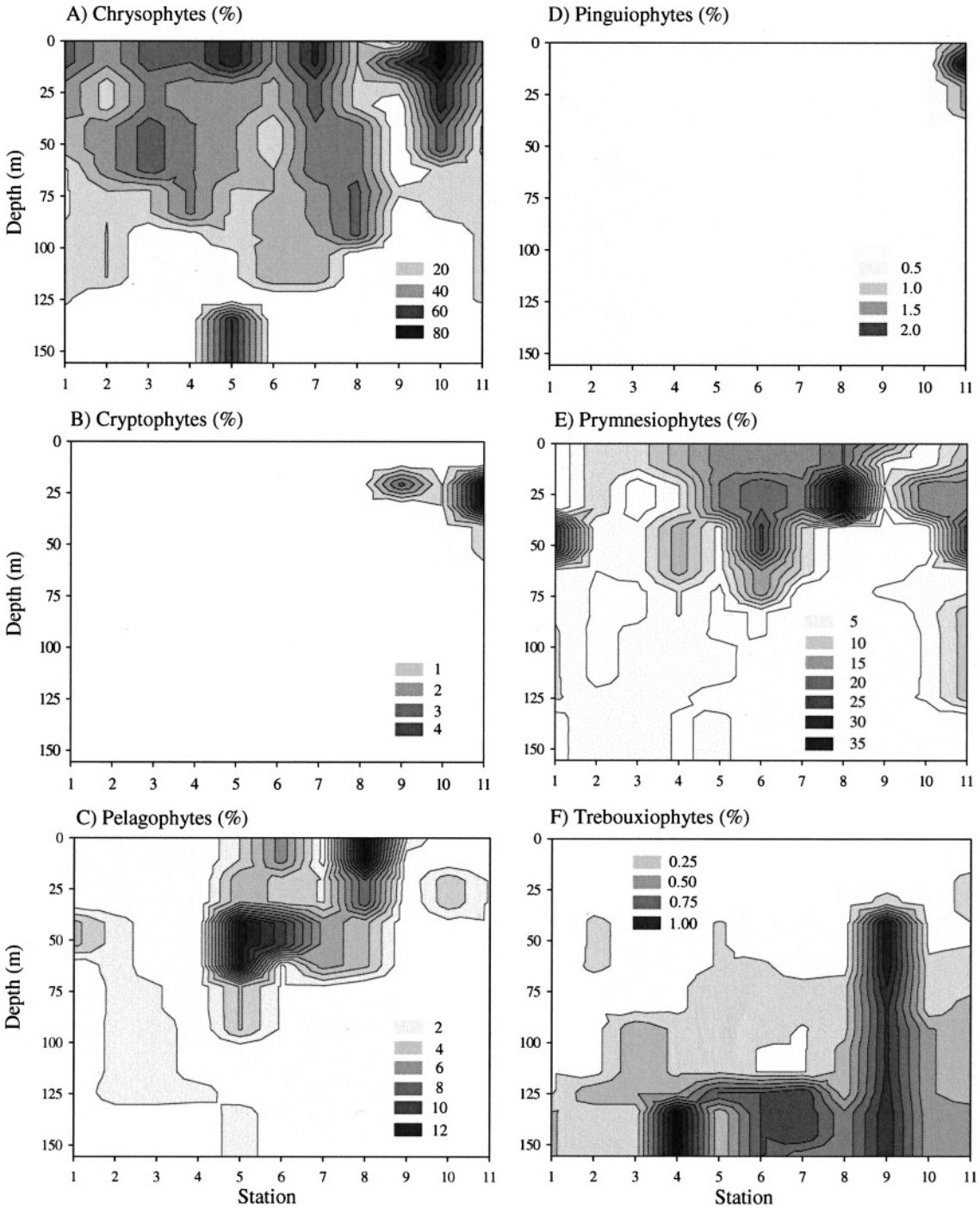

Fig. 6. Contour plots of the Arabian Sea transect, from Sta. 1 in the south to Sta. 11 in the north, of photosynthetic picoeukaryotes, as % relative hybridization (as a proportion of all amplified by primers PLA491F and OXY1313R). (A) Chrysophytes, (B) cryptophytes, (C) pelagophytes, (D) pinguiophytes, (E) prymnesiophytes, and (F) trebouxiophytes.

Sta. 8 (13.8% ± 0.3%). Pinguiophytes were detected only with low signal, reaching a maximum of 2.2% ± 0.1% (Sta. 11, 10 m), but their distribution was clearly defined, being restricted to shallow, warm surface waters at Sta. 11 (Fig. 6D), where the temperature exceeded 31°C. Prymnesiophytes were abundant in surface waters along much of the transect (Fig. 6E), contributing the second greatest proportion to total algal signal, after chrysophytes, with a maximum signal of 39.5% ± 1.9% at the DCM of Sta. 8. Although the signal from trebouxiophytes was very low, reaching a maximum of 1.2% ± 0.1% (Sta. 4, 150 m), their distribution was also very distinct, being confined to deeper waters, below the SML (Fig. 6F). Indeed, trebouxiophytes were detected as deep as 200 m at Sta. 6 (0.7% ± 0.1%) and 280 m at Sta. 5 (0.3% ± 0.1%) (data not shown). Both these deep samples were taken because a minor peak in Chl

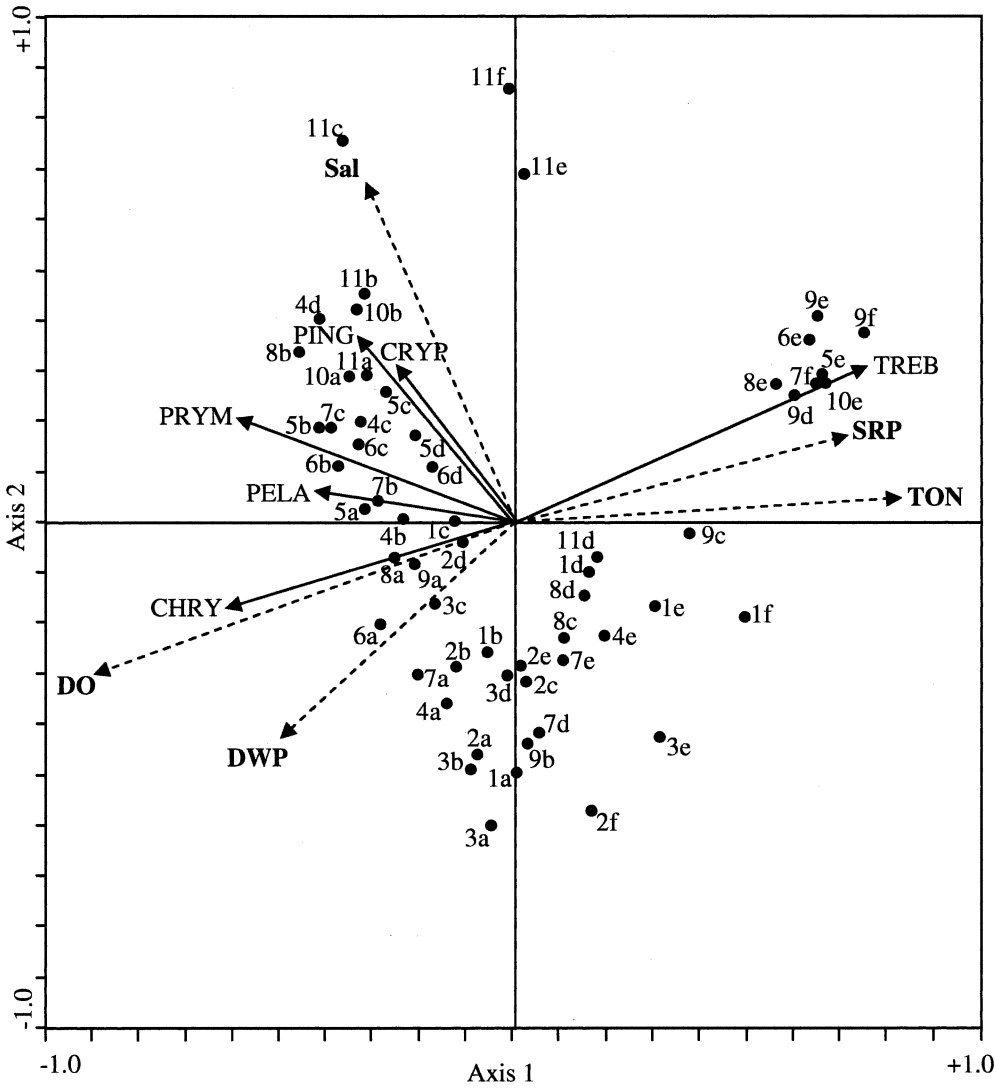

Fig. 7. RDA ordination diagram of photosynthetic picoeukaryote dot blot hybridization data obtained from PLA491F–OXY1313R PCR amplicons (solid lines), environmental variables, and pigment data (dotted lines). Arrows show the approximate linear correlation coefficients between the PPE classes and environmental variables. Data points for sites are labeled with the number according to the sampling station (*see* Fig. 1). The associated letters represent depths in the profile, with 'a' being the shallowest sample from a particular station. SRP = soluble reactive phosphate, TON = total oxidizable nitrogen, Sal = salinity, DWP = downwelling photosynthetically active radiation (PAR), DO = dissolved oxygen, PELA = pelagophytes, PRYM = prymnesiophytes, PING = pinguiophytes, CHRY = chrysophytes, CRYP = cryptophytes, and TREB = trebouxiophytes. Arrows pointing in roughly the same direction indicate a high positive correlation, arrows crossing at right angles indicate a near-zero correlation, and arrows pointing in the opposite direction have a high negative correlation.

a fluorescence was observed at these depths (0.11 and 0.08 mg m^{-3}, respectively) (data not shown). Eustigmatophytes, pavlovophytes, and clade VI prasinophytes were not detected anywhere in the transect. Chlorarachniophytes were detected only at the surface (10 m) of Sta. 10, and with a very low signal (0.12% ± 0.01%) (data not shown).

Multivariate analysis—Axis 1 of the RDA triplot (Fig. 7) showed a strong nutrient gradient, with sites to the right of the ordination representing those from the northern, deeper, and more meso-eutrophic waters. Sites close to Axis 1 on the left of the plot are mostly surface waters from sites in the southern or mid- portion of the transect characterized by relatively more oligo- or mesotrophic conditions and higher oxygen saturation concentrations. Species located toward the edge of the ordination (e.g., trebouxiophytes) were more important indicators of site differences than those located close to the center (e.g., pelagophytes). Trebouxiophytes were located to the right, with their distribution restricted to the deeper, nutrient-

rich, coastal waters. All other algal groups were positioned to the left of the ordination. Chrysophytes showed a strong correlation with sites with relatively high dissolved oxygen concentrations and higher irradiance. Pelagophytes and prymnesiophytes occupied a similar position adjacent to Axis 1, showing a negative correlation with trebouxiophytes and indicating their presence in waters of lower nutrient concentration. Axis 2 is a salinity gradient, and both the pinguiophytes and cryptophytes correlate positively with higher salinities. The first two axes represented 89% of the information explained by the five explanatory variables. However, only 34% of the total species variance was explained.

Correlations between PPEs and pigments—No significant correlations were found between the various pigment groups and either the chrysophytes or pinguiophytes. Strong ($p \leq 0.001$) positive correlations were found between the pelagophytes and two pigment groups, 19BF and 19HF, and good positive correlations were recorded for fucoxanthin and peridinin with this algal group ($p < 0.01$). A positive correlation was found between cryptophytes and peridinin ($p \leq 0.01$) and between prymnesiophytes and 19HF and peridinin ($p \leq 0.01$). Negative correlations were found between trebouxiophytes and 19BF, 19HF, and peridinin ($p < 0.01$).

Discussion

The development of a PCR biased toward algal plastids in the marine environment (Fuller et al. 2006) was a significant step forward in permitting the assessment of marine PPE diversity, particularly in oligotrophic open-ocean habitats, which are numerically dominated by picocyanobacteria. The development of 10 algal class-specific probes in this study further permits the detailed assessment of marine PPE community structure. Classes that have only been discovered in recent years, such as Pinguiophyceae (Kawachi et al. 2002*b*), can now be detected and their distribution monitored by molecular methods. However, caution should be exercised regarding data from the cryptophyte and the pavlovophyte probes, since the former will potentially detect dinoflagellates of the genus *Dinophysis*, which have plastids similar to cryptophyte plastids (Hackett et al. 2003). The observed experimental cross-reactivity of the pavlovophyte probe is, however, not problematic if the PRAS826 probe is also used to quantify clade VI prasinophytes. In this case, with the appropriate controls, the clade VI prasinophyte signal to be expected from the pavlovophyte probe (PAVL665) can be calculated and subtracted from the PAVL665 signal.

The Arabian Sea is well known as a diverse marine environment, encompassing a wide range of physical and chemical conditions (Burkill et al. 1993), with the north being strongly influenced by biannual monsoons that blow alternately from the southwest between June and September and from the northeast between November and March. These monsoons create upwelling along the southeastern coast of Oman, making the surface waters of the northwest of the Arabian Sea meso- to eutrophic. By contrast, the southern Arabian Sea is little affected by the monsoons, with relatively stable stratification of the water column, leading to highly oligotrophic conditions typical of open-ocean gyres. The transect sampled in this study crossed such a range of environmental conditions (Fig. 3), as the northern waters were reached shortly after the southwestern monsoon, thus encountering areas of high productivity, compared with the low-chlorophyll waters in the open ocean further south (Fig. 4). As expected, PPE abundance was lower in the more nutrient-poor south, which was dominated numerically by picocyanobacteria, and greater in the more nutrient-rich north. Such a trend is a common observation for PPEs (*see*, for example, Partensky et al. 1996; Brown et al. 1999).

Using the tools developed in this and a previous study (Fuller et al. 2006) we report, for the first time, molecular analysis of the community structure of selected PPEs along an oceanic transect. Interestingly, the most abundant PPE group was chrysophytes (Fig. 6A), which were predominantly associated with warmer surface waters, where irradiance levels were high (Fig. 7), although they were also found below the photic zone. This abundance is surprising given that there are relatively few reports of this algal class in marine systems. Thus, although there are indirect reports of chrysophytes in the open ocean, as indicated by pigment studies (Mackey et al. 1998), previous molecular work, particularly the construction of 18S rDNA picoplankton clone libraries from the North Atlantic and Mediterranean Sea, has indicated the presence only of heterotrophic chrysophytes (e.g., sequences closely related to *Paraphysomonas* [Diez et al. 2001]), although members of this genus can contain a nonphotosynthetic plastid remnant (or leucoplast). Similarly, those chrysophytes that have been isolated from open-ocean sites appear to be solely heterotrophic (e.g., *Picophagus* sp. [*see* Guillou et al. 1999; Vaulot et al. 2004]). The exceptions to the relative dearth of information on marine chrysophytes are reports of members of the order Parmales in polar and subpolar waters (Booth and Marchant 1987) as well as in tropical regions (Bravo-Sierra and Hernández-Becerril 2003). The Parmales encompass a group of small (<5 μm in diameter), siliceous cells, each with a chloroplast. Unfortunately, the lack of cultured representatives of this order prevents the identification of environmental plastid 16S rRNA gene sequences obtained from this Arabian Sea transect (Fuller et al. 2006) with members of this order. We should point out, though, that the dot blot hybridization data presented here would be sensitive to the number of ribosomal operons per plastid genome as well as plastid number per cell. Hence, the relative hybridization data presented here for chrysophytes, as well as the other PPE classes, needs to be viewed with some caution, especially when attempting to equate the data with abundance estimates. The application of fluorescent in situ hybridization (FISH) (e.g., *see* Not et al. 2002) or quantitative PCR technology (e.g., *see* Zhu et al. 2005; Countway and Caron 2006) will be crucial for a more accurate assessment of relative abundance.

The detection of trebouxiophytes at the bottom of the euphotic zone (Fig. 6F) is also surprising, as members of

this class are not known to possess pigments capable of giving them a selective growth advantage over picocyanobacteria at such low light intensities. Isolation and characterization of these organisms would therefore be of great interest. It is possible that the TREB708 probe is detecting heterotrophic trebouxiophytes possessing nonphotosynthetic leucoplasts, such as *Prototheca* (e.g., *see* Borza et al. 2005). However, the detection of trebouxiophytes at 280 m and 200 m at Sta. 5 and 6 coincided with a peak in fluorescence of Chl *a*, indicating that there were indeed some phototrophs present. The trebouxiophytes showed a negative correlation with downwelling irradiance (Fig. 7), which may indicate a specialized survival strategy possibly akin to certain members of the Pelagophyceae (e.g., *Aureococcus anophagefferens*, a species capable of long-term dark survival) (Popels and Hutchins 2002). It is also possible that some of these Trebouxiophyceae may be particle associated. Trebouxiophytes and chrysophytes were detected at depths at which flow cytometric counts for PPEs were zero, such as Sta. 5, 150 m. It is possible that these signals may therefore have arisen from heterotrophic members of these classes (*see* above). Or, more likely, this may simply reflect the greater sensitivity of PCR compared with flow cytometry.

The total signal from all algal probes together was often less than 100% in any given sample. This likely reflects the presence of other algal classes for which we have no probes, such as Bolidophyceae, Dictyochophyceae, prasinophytes of other clades, or an as-yet-undiscovered class. Indeed, a dictyochophyte clone and several clade II prasinophyte (*Ostreococcus*) clones were recovered from a 16S rDNA library from Sta. 2, 50 m (Fuller et al. 2006), and bolidophyte RUBISCO sequences have been recovered from Sta. 5 and 6 (Wyman unpubl. data). However, the presence of picocyanobacterial and heterotrophic bacterial sequences among the PCR products cannot be ruled out, the former certainly being amplified when these are numerically abundant (Fuller et al. 2006).

The pigment data in this study are in broad agreement with those from a similar transect in the Arabian Sea during the autumn of 1994, which showed 19HF (prymnesiophytes) as abundant in the southern oligotrophic region and both 19HF and fucoxanthin (representative of diatoms) abundant in the northern nutrient-rich region (Barlow et al. 1999). While fucoxanthin is present in stramenopiles other than diatoms, diatoms were identified by microscopy and flow cytometry as dominating the phytoplankton biomass at these nutrient-rich sites (Tarran et al. 1999) and were similarly identified as abundant at the northerly stations during September 2001 (Widdicombe unpubl. data). The pigment data in this study arose from total phytoplankton, rather than just the picoplanktonic fraction, explaining some of the differences between these and the PPE molecular data. Yet there are obvious correlations, such as a prymnesiophyte relative hybridization peak at Sta. 8, 28 m (Fig. 6E) coinciding with a peak in the carotenoid 19HF (present only in prymnesiophytes and some dinoflagellates) (Fig. 5B), perhaps indicating that much of the 19HF in this sample arose from prymnesiophytes <3 μm in size. While some dinoflagellates with plastids similar to prymnesiophyte plastids also produce 19HF (Tengs et al. 2000), these would not be detected by the PRYM666 probe, as a result of four mismatches. The 19HF at the DCMs of Sta. 1 to 4, where the prymnesiophyte relative hybridization signal was not so great, could be explained by such dinoflagellates, by larger prymnesiophytes, or simply by other algae dominating the algal pigment products, such as chrysophytes and clade II prasinophytes (*Ostreococcus*). Indeed, violaxanthin (present in prasinophytes, as well as chlorophytes and eustigmatophytes) was detected at the DCMs of Sta. 3 and 4 (Fig. 5E). The proximity of prymnesiophytes and pelagophytes (Fig. 7) indicates similar environmental preferences typifying the illuminated central regions of the transect. However, only 34% of the total species variance could be explained by the environmental variables, and other key variables that determine the distribution of these picoeukaryotic groups have yet to be identified. Cryptophyte relative hybridization distribution data (Fig. 6B) corresponded well to areas of alloxanthin occurrence (present only in cryptophytes) in the north of the transect (Fig. 5A). Interestingly, cryptophytes were not detected in other regions of alloxanthin presence, perhaps indicating that this alloxanthin came from cryptophytes >3 μm in size. Furthermore, cryptophytes were detected at Sta. 9, 20 m, where alloxanthin was not detected. This may represent heterotrophic cryptophytes possessing leucoplasts, or perhaps, more likely, photoautotrophic members lacking alloxanthin. Though the CRYP862 probe detects dinoflagellates of the genus *Dinophysis*, these are unlikely to account for the signal at Sta. 9, since they are known to possess alloxanthin (Schnepf and Elbrächter 1988).

The molecular data of PPE community structure in this study build considerably on our previous knowledge. Most studies of PPEs have not dissected them into their different classes; rather, they simply looked at this group as a whole. The few molecular studies of PPE community structure have focused on coastal regions, while open-ocean oligotrophic regions have largely been ignored, partly because of the difficulty of identifying PPEs among the much more numerous picocyanobacteria *Prochlorococcus* and *Synechococcus*. 18S rRNA FISH studies in coastal waters of northern France revealed the PPEs to be dominated by prasinophytes, particularly of the order Mamiellales, with haptophytes, pelagophytes, and bolidophytes also present, but to a lesser extent (Not et al. 2002, 2004; Biegala et al. 2003). This study showed that in coastal waters of the northern Arabian Sea, prymnesiophytes and, to a lesser extent, pelagophytes were also detected (Fig. 6). However, a lack of specific probes meant that we were unable to determine whether members of the Mamiellales or bolidophytes were also present. Pelagophytes have also been found to be among the major eukaryotic phytoplankton in the equatorial Pacific Ocean (Bidigare and Ondrusek 1996). This agrees well with our observations of pelagophytes in the more mesotrophic waters along the AMBITION cruise transect. Pelagophyte 18S rDNA sequences have also been obtained from the equatorial Pacific (Moon-Van Der Staay et al. 2001) and Mediterranean Sea (Diez et al. 2001). 16S rDNA sequences, which we are now able to identify as pelagophytes, were also common in two clone libraries from the Southern Ocean

(Wilmotte et al. 2002). In the few picoplanktonic 18S rDNA clone libraries made so far, prasinophyte (clade VII) and prymnesiophyte sequences were found to be relatively abundant in the oligotrophic equatorial Pacific Ocean, although dictyochophyte and pelagophyte sequences were also detected (Moon-Van Der Staay et al. 2000, 2001; Romari and Vaulot 2004). Such abundance of prymnesiophytes corresponds nicely with the molecular data presented here, but for clade VII prasinophytes, a specific 16S rDNA oligonucleotide probe remains to be developed.

The presence of cryptophytes of <3 μm in the more coastal and nutrient-rich northern waters in this study (Fig. 6B) is in agreement with the results of a previous study, which identified cryptophytes of picoplanktonic size in the more nutrient-rich coastal waters of northern France (Romari and Vaulot 2004). Our observation of pinguiophytes in warm, coastal surface waters in the northern Arabian Sea represents the first time pinguiophytes have been identified in the marine environment by molecular methods, although there are previous marine isolates. Indeed, a picoplanktonic form was isolated from surface waters of the tropical western Pacific Ocean (Kawachi et al. 2002*a*). Yet, until now, we had no idea as to the actual distribution of this class in marine systems.

The development of oligonucleotide probes targeting 10 algal classes, combined with a recently developed marine algal-biased PCR (Fuller et al. 2006), has enabled for the first time a detailed study of marine PPE community structure across a range of environmental conditions in the Arabian Sea. This study forms an essential basis for extending our understanding of these ecologically important phototrophs. Further use of these molecular tools, in combination with PCR-independent techniques such as FISH, will be necessary to help elucidate the role of individual PPE classes in global carbon fixation.

References

Altschul, S. F., and others. 1997. Gapped BLAST and PSI-BLAST: A new generation of protein database search programs. Nucl. Acids Res. **25:** 3389–3402.

Barlow, R. G., D. G. Cummings, and S. W. Gibb. 1997. Improved resolution of mono- and divinyl chlorophylls a and b and zeaxanthin and lutein in phytoplankton extracts using reverse phase C-8 HPLC. Mar. Ecol. Prog. Ser. **161:** 303–307.

———, R. F. C. Mantoura, and D. G. Cummings. 1999. Monsoonal influence on the distribution of phytoplankton pigments in the Arabian Sea. Deep-Sea Res. II **46:** 677–699.

Bidigare, R. R., and M. E. Ondrusek. 1996. Spatial and temporal variability of phytoplankton pigment distributions in the central equatorial Pacific Ocean. Deep-Sea Res. II **43:** 809–833.

Biegala, I. C., F. Not, D. Vaulot, and N. Simon. 2003. Quantitative assessment of picoeukaryotes in the natural environment by using taxon-specific oligonucleotide probes in association with tyramide signal amplification-fluorescence in situ hybridization and flow cytometry. Appl. Environ. Microbiol. **69:** 5519–5529.

Blanchot, J., J. M. Andre, C. Navarette, J. Neveux, and M. H. Radenac. 2001. Picophytoplankton in the equatorial Pacific: Vertical distributions in the warm pool and in the high nutrient low chlorophyll conditions. Deep-Sea Res. I **48:** 297–314.

Booth, B. C., and H. J. Marchant. 1987. Parmales, a new order of marine chrysophytes, with descriptions of three new genera and seven new species. J. Phycol. **23:** 245–260.

Borza, T., C. E. Popescu, and R. W. Lee. 2005. Multiple metabolic roles for the nonphotosynthetic plastid of the green alga *Prototheca wickerhamii*. Eukaryotic Cell **4:** 253–261.

Bravo-Sierra, E., and D. U. Hernández-Becceril. 2003. Parmales (Chrysophyceae) from the Gulf of Tehuantepec, Mexico, including the description of a new species, *Tetraparma insecta* sp. nov., and a proposal to the taxonomy of the group. J. Phycol. **39:** 577–583.

Brewer, P. G., and J. P. Riley. 1965. The automatic determination of nitrate in seawater. Deep-Sea Res. **12:** 765–772.

Brown, S. L., M. R. Landry, R. T. Barber, L. Campbell, D. L. Garrison, and M. M. Gowing. 1999. Picophytoplankton dynamics and production in the Arabian Sea during the 1995 Southwest Monsoon. Deep-Sea Res. II **46:** 1745–1768.

Burkill, P. H., R. F. C. Mantoura, and N. J. P. Owens. 1993. Biogeochemical cycling in the northwestern Indian Ocean: A brief overview. Deep-Sea Res. II **40:** 643–649.

Countway, P. D., and D. A. Caron. 2006. Abundance and distribution of *Ostreococcus* sp. in the San Pedro Channel, California, as revealed by quantitative PCR. Appl. Environ. Microbiol. **72:** 2496–2506.

Diez, B., C. Pedros-Alio, and R. Massana. 2001. Study of genetic diversity of eukaryotic picoplankton in different oceanic regions by small-subunit rRNA gene cloning and sequencing. Appl. Environ. Microbiol. **67:** 2932–2941.

Edwards, U., T. Rogall, H. Blocker, M. Emde, and E. C. Bottger. 1989. Isolation and direct complete nucleotide determination of entire genes. Characterization of a gene coding for 16S ribosomal RNA. Nucl. Acids Res. **17:** 7843–7853.

Fuller, N. J., D. Marie, F. Partensky, D. Vaulot, A. F. Post, and D. J. Scanlan. 2003. Clade-specific 16S ribosomal DNA oligonucleotides reveal the predominance of a single marine *Synechococcus* clade throughout a stratified water column in the Red Sea. Appl. Environ. Microbiol. **69:** 2430–2443.

———, N. J. West, D. Marie, M. Yallop, T. Rivlin, A. F. Post, and D. J. Scanlan. 2005. Dynamics of community structure and phosphate status of picocyanobacterial populations in the Gulf of Aqaba, Red Sea. Limnol. Oceanogr. **50:** 363–375.

———, and others. 2006. Analysis of photosynthetic picoeukaryote diversity at open ocean sites in the Arabian Sea using a PCR biased towards marine algal plastids. Aquat. Microb. Ecol. **43:** 79–93.

Groben, R., U. John, G. Eller, M. Lange, and L. K. Medlin. 2004. Using fluorescently-labelled rRNA probes for hierarchial estimation of phytoplankton diversity. Nova Hedwigia **79:** 313–320.

Guillou, L., M.-J. Chretiennot-Dinet, S. Boulben, S-Y Moon-van der Staay, and D. Vaulot. 1999. *Symbiomonas scintillans* gen. et sp. nov. and *Picophagus flagellatus* gen. et sp. nov. (Heterokonta): Two new heterotrophic flagellates of picoplanktonic size. Protist **150:** 383–398.

———, and others. 2004. Diversity of picoplanktonic prasinophytes assessed by direct nuclear SSU rDNA sequencing of environmental samples and novel isolates retrieved from oceanic and coastal marine ecosystems. Protist **155:** 193–214.

HACKETT, J. D., L. MARANDA, H. S. YOON, AND D. BHATTACHARYA. 2003. Phylogenetic evidence for the cryptophyte origin of the plastid of *Dinophysis* (Dinophysiales, Dinophyceae). J. Phycol. **39:** 440–448.

HOOKS, C. E., R. R. BIDIGARE, M. D. KELLER, AND R. R. L. GUILLARD. 1988. Coccoid eukaryotic marine ultraplankters with four different HPLC pigment signatures. J. Phycol. **24:** 571–580.

JONES, R. D. 1991. An improved fluorescence method for the determination of nanomolar concentrations of ammonium in natural waters. Limnol. Oceanogr. **36:** 814–819.

KAWACHI, M., M. ATSUMI, H. IKEMOTO, AND S. MIYACHI. 2002*a*. *Pinguiochrysis pyriformis* gen. et sp. nov. (Pinguiophyceae), A new picoplanktonic alga isolated from the Pacific Ocean. Phycol. Res. **50:** 49–56.

———, I. INOUYE, D. HONDA, C. J. O'KELLY, J. C. BAILEY, R. R. BIDIGARE, AND R. A. ANDERSEN. 2002*b*. The Pinguiophyceae *classis nova*, a new class of photosynthetic stramenopiles whose members produce large amounts of omega-3 fatty acids. Phycol. Res. **50:** 31–47.

KIRKWOOD, D. 1989. Simultaneous determination of selected nutrients in sea water. International Council for the Exploration of the Sea (ICES) CM 1989/C **29:** 12 pp.

LI, W. K. W. 1994. Primary production of prochlorophytes, cyanobacteria, and eukaryotic ultraphytoplankton: Measurements from flow cytometric sorting. Limnol. Oceanogr. **39:** 169–175.

LUDWIG, W., AND OTHERS. 2004. ARB: A software environment for sequence data. Nucl. Acids Res. **32:** 1363–1371.

MACKEY D. J., H. W. HIGGINS, M. D. MACKEY, AND D. HOLDSWORTH. 1998. Algal class abundances in the western equatorial Pacific: Estimation from HPLC measurements of chloroplast pigments using CHEMTAX. Deep-Sea Res. I **45:** 1441–1468.

MOON-VAN DER STAAY, S. Y., R. DE WACHTER, AND D. VAULOT. 2001. Oceanic 18S rDNA sequences from picoplankton reveal unsuspected eukaryotic diversity. Nature **409:** 607–610.

———, G. W. M. VAN DER STAAY, L. GUILLOU, D. VAULOT, H. CLAUSTRE, AND L. K. MEDLIN. 2000. Abundance and diversity of prymnesiophytes in the picoplankton community from the equatorial Pacific Ocean inferred from 18S rDNA sequences. Limnol. Oceanogr. **45:** 98–109.

NOT, F., M. LATASA, D. MARIE, T. CARIOU, D. VAULOT, AND N. SIMON. 2004. A single species, *Micromonas pusilla* (Prasinophyceae), dominates the eukaryotic picoplankton in the western English Channel. Appl. Environ. Microbiol. **70:** 4064–4072.

———, N. SIMON, I. C. BIEGALA, AND D. VAULOT. 2002. Application of fluorescent in situ hybridization coupled with tyramide signal amplification (FISH-TSA) to assess eukaryotic picoplankton composition. Aquat. Microb. Ecol. **28:** 157–166.

NÜBEL, U., F. GARCIA-PICHEL, AND G. MUYZER. 1997. PCR primers to amplify 16S rRNA genes from cyanobacteria. Appl. Environ. Microbiol. **63:** 3327–3332.

PARTENSKY, F., J. BLANCHOT, F. LANTOINE, J. NEVEUX, AND D. MARIE. 1996. Vertical structure of picophytoplankton at different trophic sites of the Tropical Northeastern Atlantic Ocean. Deep-Sea Res. I **43:** 1191–1213.

POPELS, L. C., AND D. A. HUTCHINS. 2002. Factors affecting dark survival of the brown tide alga *Aureococcus anophagefferens* (Pelagophyceae). J. Phycol. **38:** 738–744.

ROMARI, K., AND D. VAULOT. 2004. Composition and temporal variability of picoeukaryote communities at a coastal site of the English Channel from 18S rDNA sequences. Limnol. Oceanogr. **49:** 784–798.

SCHNEPF, E., AND M. ELBRÄCHTER. 1988. Cryptophycean-like double membrane-bound chloroplast in the dinoflagellate, *Dinophysis* Ehrenb.: Evolutionary, phylogenetic and toxicological implications. Bot. Acta **101:** 196–203.

TAKAHASHI, Y., K. TAKASHITA, K. KOIKE, T. MARUYAMA, T. NAKAYAMA, A. KOBIYAMA, AND T. OGATA. 2005. Development of molecular probes for *Dinophysis* (Dinophyceae) plastid: A tool to predict blooming and explore plastid origin. Mar. Biotech. **7:** 95–103.

TARRAN, G. A., P. H. BURKILL, E. S. EDWARDS, AND E. M. S. WOODWARD. 1999. Phytoplankton community structure in the Arabian Sea during and after the SW monsoon, 1994. Deep-Sea Res. II **46:** 655–676.

TENGS, T., O. J. DAHLBERG, K. SHALCHIAN-TABRIZI, D. KLAVENESS, K. RUDI, C. F. DELWICHE, AND K. S. JAKOBSEN. 2000. Phylogenetic analyses indicate that the 19′ hexanoyloxy-fucoxanthin-containing dinoflagellates have tertiary plastids of haptophyte origin. Mol. Biol. Evol. **17:** 718–729.

TER BRAAK, C. J. F. 1987. CANOCO—A FORTRAN program for canonical community ordination by partial detrended canonical correspondence analysis, principal components analysis and redundancy analysis (version 2.1). Report LWA-88-02. Agricultural Mathematics Group, Wageningen, The Netherlands.

———. 1990. Update notes: CANOCO version 3.1 Agricultural Mathematics Group, Wageningen, The Netherlands. 35 pp.

———. 1994. Canonical community ordination. Part 1. Basic theory and linear methods. Ecoscience **1:** 127–140.

VAULOT, D., F. LE GALL, D. MARIE, L. GUILLOU, AND F. PARTENSKY. 2004. The Roscoff Culture Collection (RCC): A collection dedicated to marine picoplankton. Nova Hedwigia **79:** 49–70.

WEST, N. J., W. A. SCHÖNHUBER, N. J. FULLER, R. I. AMANN, R. RIPPKA, A. F. POST, AND D. J. SCANLAN. 2001. Closely related *Prochlorococcus* genotypes show remarkably different depth distributions in two oceanic regions as revealed by in situ hybridisation using 16S rRNA-targeted oligonucleotides. Microbiology **147:** 1731–1744.

WILMOTTE, A. D., C. DEMONCEAU, A. GOFFART, J.-H. HECQ, V. DEMOULIN, AND A. C. CROSSLEY. 2002. Molecular and pigment studies of the picophytoplankton in a region of the Southern Ocean (42–54°S, 141–144°E) in March 1998. Deep-Sea Res. II **49:** 3351–3363.

WOODWARD, E. M. S. 2002. Nanomolar detection for phosphate and nitrate using liquid waveguide technology. 2002 Ocean Sciences Meeting. Eos Trans. Am. Geophys. Union **83:** 92.

———, A. P. REES, AND J. A. STEPHENS. 1999. The influence of the South-West monsoon upon the nutrient biogeochemistry of the Arabian Sea. Deep-Sea Res. II **46:** 571–591.

WORDEN, A. Z., J. K. NOLAN, AND B. PALENIK. 2004. Assessing the dynamics and ecology of marine picophytoplankton: The importance of the eukaryotic component. Limnol. Oceanogr. **49:** 168–179.

ZHU, F., R. MASSANA, F. NOT, D. MARIE, AND D. VAULOT. 2005. Mapping of picoeukaryotes in marine ecosystems with quantitative PCR of the 18S rRNA gene. FEMS Microbiol. Ecol. **52:** 79–92.

Received: 15 December 2005
Accepted: 27 June 2006
Amended: 4 July 2006